Dendrimer Sensors

DOI: 10.1002/anie.200602858

Click Assembly of 1,2,3-Triazole-Linked Dendrimers, Including Ferrocenyl Dendrimers, Which Sense Both Oxo Anions and Metal Cations**

*Cátia Ornelas, Jaime Ruiz Aranzaes, Eric Cloutet, Sandra Alves, and Didier Astruc**

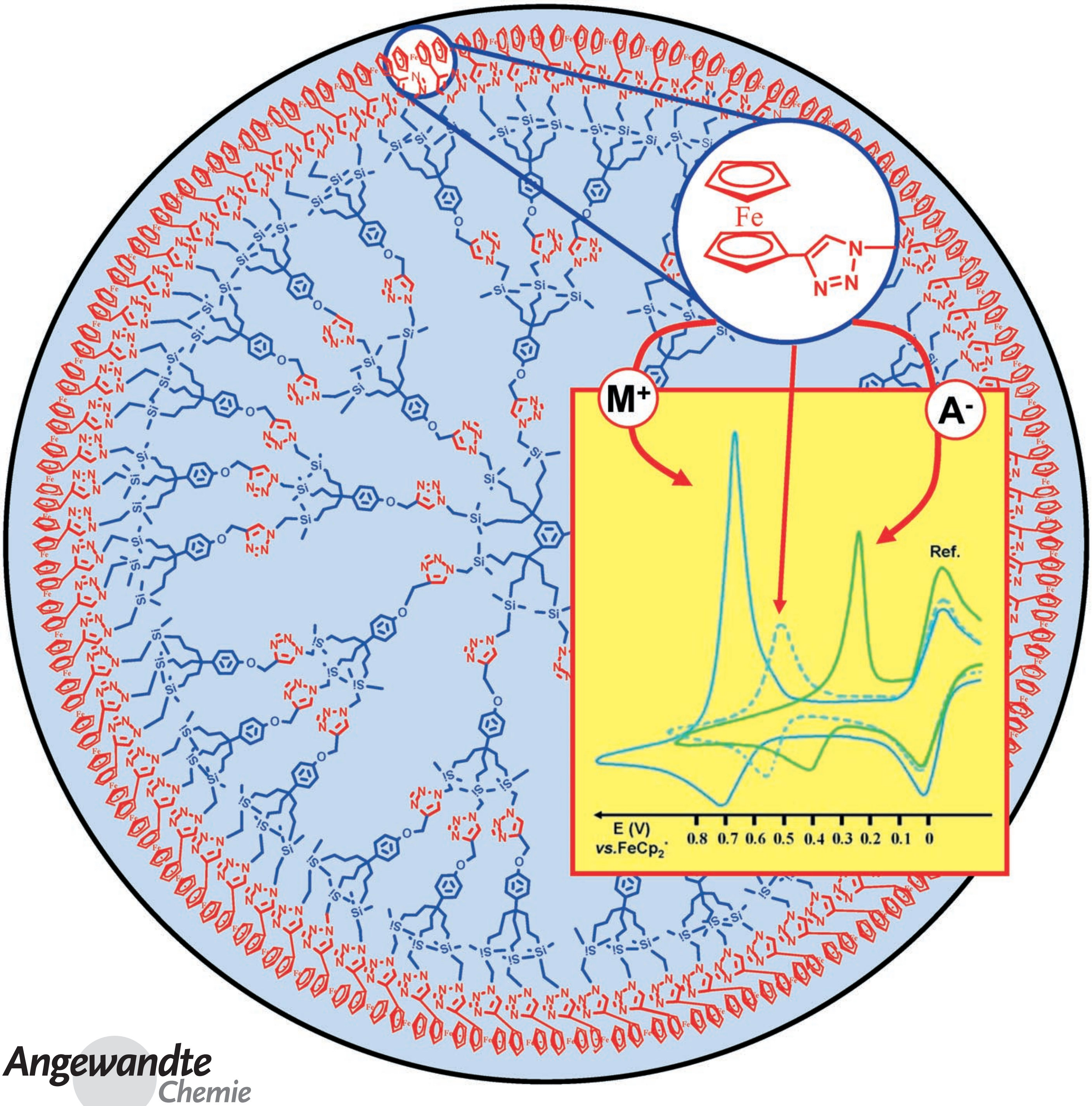

Dendrimers are well-defined macromolecules[1] whose multifaceted supramolecular properties can be applied to various fields of nanoscience, such as vectors, sensors, and green catalysts.[1,2] We have now assembled dendrimers linked by 1,2,3-triazole heterocycles by the Huisgen 1,3-dipolar cycloaddition between azides and alkynes, a reaction that has recently been greatly improved and defined by Sharpless as "click chemistry" because of its regioselectivity and catalytic course in the presence of Cu^I, its tolerance of a wide range of functionalities, and its high yields in water.[3] Recently there have been a few reports of the linkage of dendrons to cores using click reactions.[4] Our goal was threefold: 1) to investigate the full click assembly of 9-, 27-, and 81-tethered dendrimers; 2) to functionalize these dendrimers with a ferrocenyl group also by click chemistry; and 3) to investigate the ability of the 1,2,3-triazole rings located inside these metallodendrimers to recognize, bind, and sense oxo anions and metal cations using the ferrocenyl termini as a redox monitor[2b] directly attached to the triazole ring.

For the construction of the dendrimers (Scheme 1) we used the 1→3 C connectivity pioneered by Newkome.[5] The known nona-allylation of $[FeCp(\eta^6\text{-mesitylene}](PF_6)$ (**1**; $Cp = C_5H_5$) quantitatively yielded the nona-allyl dendritic core **2** on a large scale after visible-light photolysis to remove the metal moiety.[6] Likewise, the known triallyl–phenol dendronic brick *para*-$HOC_6H_4\{C(CH_2CH{=}CH_2)_3\}$, obtained from the one-pot reaction of $[FeCp(\eta^6\text{-}para\text{-ethoxytoluene})](PF_6)$ with allyl bromide and *t*BuOK,[6] was synthesized to serve as the precursor of the building block used for dendritic progression.

Hydrosilylation of the terminal olefinic bonds of **2**, a reaction pioneered in dendrimer synthesis by van Leeuwen et al.,[7] was carried out with $HSiMe_2(CH_2Cl)$, the Karsted catalyst, to give the nona-chloromethyl(dimethyl)silyl intermediate regioselectively, which, upon treatment with NaN_3, provided the nona-azide **4**. Functionalization of the triallyl–phenol dendron with propargyl bromide at the phenol focal point gave dendron **5**, which is suitable for click chemistry. The Cu^I-induced click reaction between **4** and **5** in water/THF yielded the first-generation (G_1) 27-allyl dendrimer **6**, which contains nine 1,2,3-triazole links and was characterized by its molecular peak at 3937.42 $[M+Na^+]$ in the MALDI-TOF mass spectrum (calcd for $C_{234}H_{327}N_{27}O_9Si_9Na$: 3938.04). Repetition of this sequence of reactions yielded the 27-azido intermediate **8** and subsequently the 81-allyl second-generation (G_2) dendrimer **9**, which contains 36 triazole links in two layers (9 + 27).

Note that whereas this click reaction is usually catalytic with Cu^I (5% Cu^I is used by most authors), the present click dendrimer synthesis requires a stoichiometric amount of Cu^I because the metal remains trapped inside the dendrimer and is only removed as $[Cu(NH_3)_6]^+$ ions by washing with aqueous ammonia solution. This feature was further confirmed by recognition and titration studies of the click dendrimers with Cu^I (see below). On the other hand, an advantage of this procedural variation is that our click reaction is much faster than the standard procedure (0.5 h at 20 °C instead of 16 h).

To monitor the functions of the triazole groups, such as molecular recognition or metal complexation, by cyclic voltammetry (CV), we attached ferrocenyl groups to the triazole units at the periphery of the dendrimers by treating the polyazido dendrimers **4**, **8**, and **11** (generations G_0, G_1, and G_2, respectively) with ethynylferrocene ($FcC{\equiv}CH$) to yield the poly-1,2,3-triazolylferrocenyl dendrimers **12**, **13**, and **14**, respectively, under ambient conditions in water/THF [Eq. (1)–(3)].

$$\text{Dendr-}(CH_2N_3)_9\ (\mathbf{4}) + FcC{\equiv}CH \rightarrow \text{Dendr-}(CH_2{-}N_3C_2H{-}Fc)_9\ (\mathbf{12}) \qquad (1)$$

$$\text{Dendr-}(CH_2N_3)_{27}\ (\mathbf{8}) + FcC{\equiv}CH \rightarrow \text{Dendr-}(CH_2{-}N_3C_2H{-}Fc)_{27}\ (\mathbf{13}) \qquad (2)$$

$$\text{Dendr-}(CH_2N_3)_{81}\ (\mathbf{11}) + FcC{\equiv}CH \rightarrow \text{Dendr-}(CH_2{-}N_3C_2H{-}Fc)_{81}\ (\mathbf{14}) \qquad (3)$$

These poly-1,2,3-triazolylferrocenyl dendrimers were characterized by ^1H, ^{13}C, 2D ^1H-^{13}C correlation, and ^{29}Si NMR spectroscopy, MALDI-TOF spectrometry (G_0, **12**), and size-exclusion chromatography (SEC). SEC (see Supporting Information, page 36) shows the size progression from G_0 (**12**) to G_2 (**14**) and the low polydispersity (1.00 to 1.02). The G_2 dendrimer **14** was also characterized by dynamic light scattering (DLS), its hydrodynamic diameter in dichloromethane solution being (12 ± 0.5) nm.

The ferrocenyl dendrimers **12**–**14** show a single, fully reversible CV wave for all the equivalent (but distant) ferrocenyl groups. The potentials of these groups are similar, the electrostatic factor apparently being very weak.[2b,8] Determination of the number of electrons included in this wave using the Bard–Anson equation[9] with decamethylferrocene as the internal reference gives 9 ± 1, 29 ± 3, and 87 ± 9 electrons for **12**, **13**, and **14** respectively, in good agreement with the theoretical numbers. The very slight excess found is probably due to a slight adsorption phenomenon, which increases as the dendrimer generation increases.

Recognition of oxo anions by ferrocenyl-based redox sensors has been studied thoroughly using various *endo*

---

[*] C. Ornelas, Dr. J. Ruiz Aranzaes, Prof. D. Astruc
Nanosciences Moléculaires et Catalyse
LCOO, UMR CNRS no. 5802
Université Bordeaux I
33405 Talence Cedex (France)
Fax: (+33) 5-4000-6646
E-mail: d.astruc@lcoo.u-bordeaux1.fr
Homepage: http://costd12.workshop.free.fr/Fer/

Dr. S. Alves
LCSOB, UMR CNRS N° 7613
Université Paris VI
75252 Paris Cedex (France)

Dr. E. Cloutet
LCPO, UMR CNRS N° 5629
Université Bordeaux I
33405 Talence Cedex (France)

[**] We are grateful to the Institut Universitaire de France (IUF, D.A.), Fundação para a Ciência e a Tecnologia (FCT), Portugal (PhD grant to C.O.), CNRS, and the Universities Bordeaux I and Paris VI for financial support.

Supporting Information for this article is available on the WWW under http://www.angewandte.org or from the author.

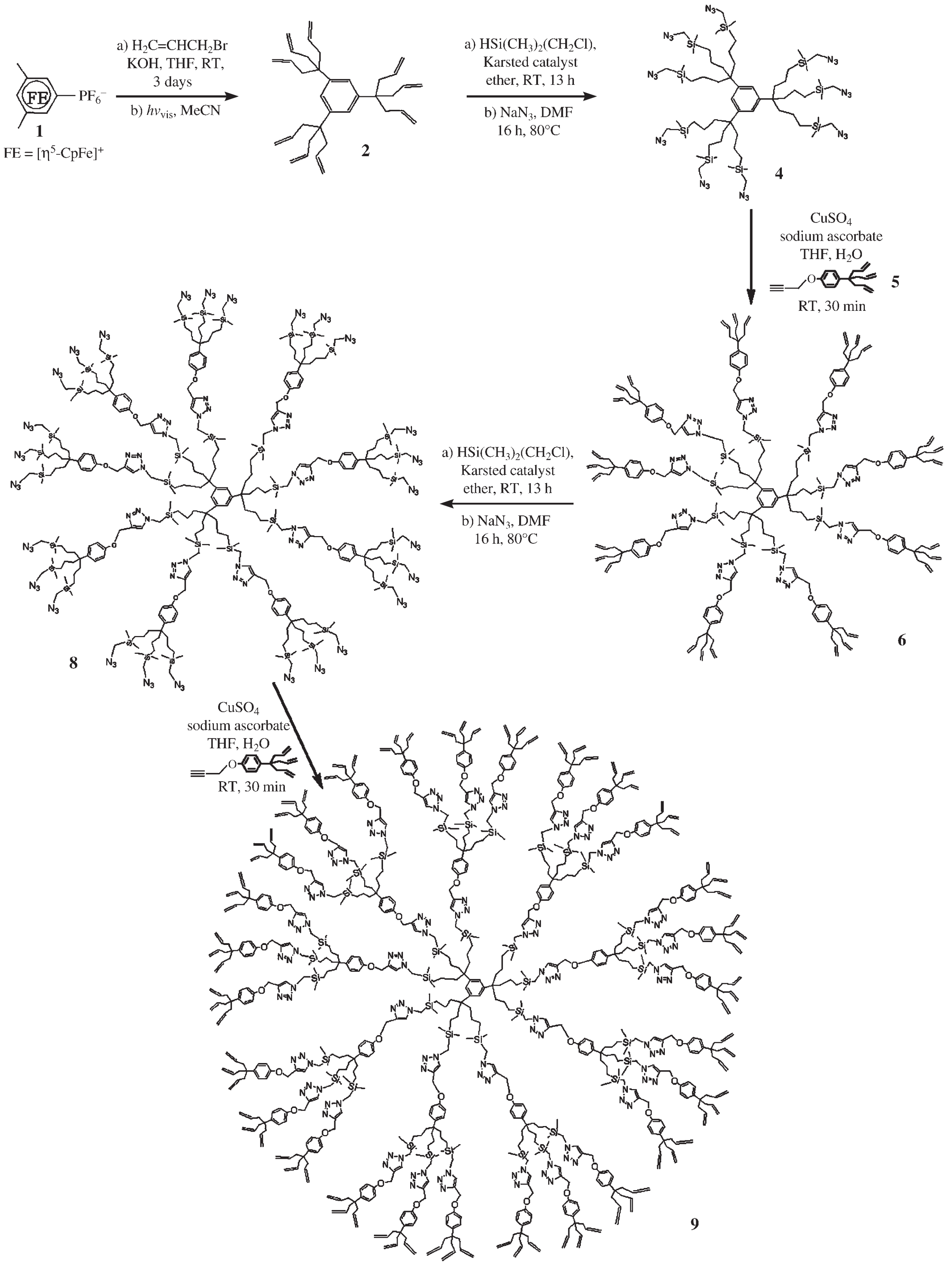

Scheme 1. Click synthesis of the 81-allyl dendrimer **9**.

receptors[10] and dendritic *exo* receptors.[2b] Very recently, Beer et al. have developed systems able to recognize both cations and anions in ion pairs using this principle.[11] The group of van Koten has also reported the use of dendrimers for efficient sensing.[2a] The ferrocenyl dendrimers **12**–**14** recognize both oxo anions and transition-metal cations by means of a new CV wave which appears when an oxo anion ($H_2PO_4^-$ or ATP^{2-}, but not HSO_4^-) or a transition-metal cation (Cu^+, Cu^{2+}, Pd^{2+}, or Pt^{2+}) salt is added to an electrochemical cell containing a CH_2Cl_2 solution of the click dendrimer (Figure 1). This result is a sign of a relatively "strong redox recognition" according to the Echegoyen–Kaifer model; a modest recognition is indicated by only a shift of the initial CV wave.[12]

For oxo anions, the new wave appears at a less positive potential than the initial wave, thus indicating that the dendrimer–oxo anion assembly is easier to oxidize than the dendrimer alone, probably because the anion donates electron density to the redox center. On the other hand, for metal cations, the new wave appears at a more positive potential than the initial wave,[13] thus showing that the cation–dendrimer assembly is more difficult to oxidize than the dendrimer alone, probably because coordination of the triazole ligand to the metal cation after MeCN ligand substitution withdraws electron density from the redox center through the triazole bridge.

This recognition by the click dendrimers indicates a dramatic positive dendritic effect, as there is no new CV wave or shift of the CV wave upon addition of the oxo anion or metal cation when the non-dendritic monoferrocenyl click model **15** [Eq. (4)] is used instead of the click dendrimers, except for Pd^{2+}.

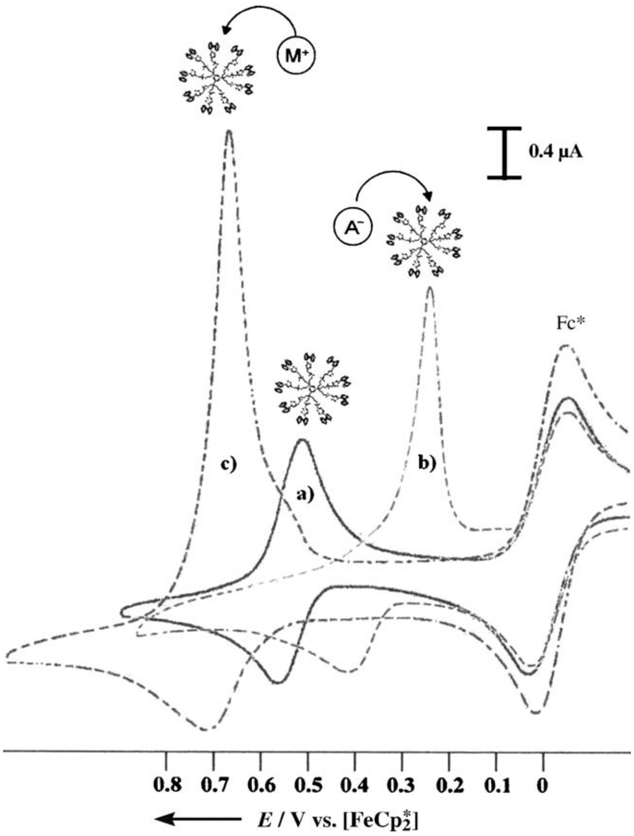

Figure 1. Redox sensing of both oxo anions (A^-)and metal cations (M^+) by poly-1,2,3-triazolylferrocenyl dendrimers: cyclic voltammograms of **12** ($c = 8.37\times10^{-5}$ м) a) without and b) in the presence of (nBu$_4$N)(H_2PO_4) (1 equiv per branch); c) cyclic voltammogram of **12** ($c = 1.26\times10^{-4}$ м) in the presence of [Pd(MeCN)$_4$](BF$_4$)$_2$ (0.25 equiv per branch). Fc*: [FeCp*$_2$], Cp* = C_5Me_5.

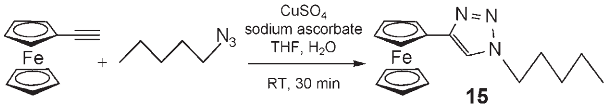

15

(4)

The recognition data are gathered in Table 1 (for the oxo anions), Table 2 (for Pd^{2+} and Pt^{2+}), and Table 3 (for Cu^+ and Cu^{2+}), which include the differences of potentials observed between the initial CV wave and the new CV wave ($\Delta E_{1/2}$), the potential difference between the new anodic and cathodic waves ($E_{pa}-E_{pc}$), and the ratios of apparent association constants ($K_{(+)}/K_{(0)}$).

For the oxo anions, the redox recognition with dendritic effect is also selective, that is, the appearance of a new wave with the click dendrimer **12** is the same with or without addition of the anions HSO_4^- or Cl^- at the same time as $H_2PO_4^-$ or ATP^{2-} (nBu$_4$N$^+$ salts). The stoichiometry of the titration corresponds to one equivalent of $H_2PO_4^-$ or half an equivalent of ATP^{2-} per ferrocenyl branch. Since *para-tert*-butylphenol (more acidic than $H_2PO_4^-$) is not recognized by these dendrimers (no CV-wave shift), we conclude that H···N hydrogen bonding between such a

Table 1: Cyclic voltammetric data for compounds **12**–**15** before and after titration with (nBu$_4$N)$_2$(ATP) or (nBu$_4$N)(H_2PO_4) in CH_2Cl_2. All energy values are given in V.

	$E_{1/2}$[a] ($E_{pa}-E_{pc}$)	i_{pc}/i_{pa}	n[b]	Recognition of ATP^{2-} $E_{1/2}$[a] ($E_{pa}-E_{pc}$)	$\Delta E_{1/2}$[c]	$K_{(+)}/K_{(0)}$[d]	Recognition of $H_2PO_4^-$ $E_{1/2}$[a] ($E_{pa}-E_{pc}$)	$\Delta E_{1/2}$[c]	$K_{(+)}/K_{(0)}$[d]
15	0.570 (0.060)	1.0	1	0.560 (0.100)	0.010	1.5	0.560 (0.100)	0.010	1.5
12	0.555 (0.050)	1.2	9	0.400 (0.140)	0.155	470	0.355 (0.140)	0.200	2807
13	0.555 (0.040)	1.8	29	0.445 (0.130)	0.110	79	0.385 (0.120)	0.170	853
14	0.555 (0.050)	1.2	87	0.465 (0.120)	0.090	36	0.400 (0.115)	0.155	470

[a] $E_{1/2} = (E_{pa} + E_{pc})/2$ vs. [FeCp*$_2$]. The peak potentials might be perturbed by some adsorption,[9b] thus $K_{(+)}/K_{(0)}$ values must be considered with caution. Adsorption is weak, however, during the titration process and becomes important only at, and after, the equivalent point. The potential of the new wave does not vary significantly during the titration or at the equivalent point. Thus, errors in the $E_{1/2}$ values are limited. Electrolyte: 0.1 м (nBu$_4$N)(PF$_6$); working and counter electrodes: Pt; quasi-reference electrode: Ag; internal reference: [FeCp*$_2$]; scan rate: 0.200 V s^{-1}; 20 °C. [b] Number of electrons involved calculated from the Anson–Bard equation[9] using anodic intensities. [c] Difference between values of $E_{1/2}$ before and after titration. [d] Ratios of apparent association constants; error < 10%; $\Delta E_{1/2} = 0.058 \log(K_{(+)}/K_{(0)})$[12] at 20 °C.

Table 2: Cyclic voltammetric data for compounds **12**–**15** before and after titration with $[Pd(MeCN)_4](BF_4)_2$ or $[Pt(MeCN)_4](BF_4)_2$ in CH_2Cl_2. All energy values are given in V.

	$E_{1/2}$[a]	Recognition of Pd^{2+}			Recognition of Pt^{2+}		
	($E_{pa}-E_{pc}$)	$E_{1/2}$ ($E_{pa}-E_{pc}$)	$\Delta E_{1/2}$[b]	$K_{(0)}/K_{(+)}$[c]	$E_{1/2}$ ($E_{pa}-E_{pc}$)	$\Delta E_{1/2}$[b]	$K_{(0)}/K_{(+)}$[c]
15	0.570 (0.060)	0.715 (0.060)	−0.145	316	0.570 (0.060)	0	–
12	0.555 (0.050)	0.705 (0.050)	−0.150	386	0.665 (0.030)	−0.110	79
13	0.555 (0.040)	0.695 (0.040)	−0.140	259	0.655 (0.020)	−0.100	53
14	0.555 (0.050)	0.690 (0.035)	−0.135	213	0.650 (0.020)	−0.095	43

For [a], [b], and [c] see footnotes [a], [c], and [d] to Table 1, respectively.

Table 3: Cyclic voltammetric data for compounds **12**–**15** before and after titration with $[Cu(MeCN)_4](BF_4)$ or $[Cu(MeCN)_4](BF_4)_2$ in CH_2Cl_2. All energy values are given in V.

	$E_{1/2}$[a]	Recognition of Cu^{2+}			Recognition of Cu^{+}		
	($E_{pa}-E_{pc}$)	$E_{1/2}$ ($E_{pa}-E_{pc}$)	$\Delta E_{1/2}$[b]	$K_{(0)}/K_{(+)}$[c]	$E_{1/2}$ ($E_{pa}-E_{pc}$)	$\Delta E_{1/2}$[b]	$K_{(0)}/K_{(+)}$[c]
15	0.570 (0.060)	0.570 (0.060)	0	–	0.570 (0.060)	0	–
12	0.555 (0.050)	0.645 (0.045)	−0.090	36	0.605 (0.030)	−0.050	7
13	0.555 (0.040)	0.635 (0.020)	−0.080	24	0.635 (0.020)	−0.080	24
14	0.555 (0.050)	0.625 (0.015)	−0.070	16	0.645 (0.015)	−0.090	36

For [a], [b], and [c] see footnotes [a], [c], and [d] to Table 1, respectively.

relatively acidic substrate and the triazole ring is insufficient to perturb the nearby ferrocenyl redox system. Thus, $H_2PO_4^-$ and ATP^{2-} ions are essentially recognized through the negatively charged oxygen atoms of the phosphato groups, which interact strongly with the Fe center when the latter is oxidized to Fe^{III} at the anode. Nevertheless, this $Fe^{\delta+}\cdots O^{\delta-}$ electrostatic perturbation of the redox center is presumably facilitated by chelation of the phosphato group through the above-mentioned N···H hydrogen bond (it is too weak in the neutral ferrocenyl form to provoke any signal shift in the ^{1}H NMR spectrum).

Contrary to all the previous redox recognition studies with both $H_2PO_4^-$ and ATP^{2-} ions and other metallodendrimers, we also observed a negative dendritic effect, that is, $\Delta E_{1/2}$ decreases slightly along the series $G_0 \rightarrow G_1 \rightarrow G_2$ for both oxo anions and metal cations, except for Cu^+ (see below). This negative dendritic effect could possibly be due to inhibiting steric effects.

The $E_{pa}-E_{pc}$ values illustrate the heterogeneous electron-transfer rates and adsorption events, and these values are completely different for oxo anions and metal cations. Whereas large $E_{pa}-E_{pc}$ values (140 mV for **12** and decreasing slightly with the dendrimer size) show the important reorganization of the dendrimer–guest assemblies upon slow heterogeneous electron transfer in the case of oxo anions, small $E_{pa}-E_{pc}$ values (30–50 mV for **12** and decreasing with dendrimer size down to 15–35 mV), which are lower than the standard value of 58 mV at 25 °C for all the transition-metal cations, indicate some adsorption onto the electrode owing to the positive charges gained by the dendrimer–cation assemblies. The increased tendency of dendrimers to adsorb onto electrodes when their size increases can be exploited for the fabrication of dendrimer-derivatized electrodes (see Supporting Information, Figure S12) that are also useful for sensing.

There are marked differences in the redox recognition features of the selected transition-metal cations: Cu^+, Cu^{2+}, and Pt^{2+} are not recognized by the model complex **15**, and the redox recognition of Cu^+ ions shows a continuously positive dendritic effect as the dendrimer generation increases (Figure 2). On the other hand, the redox recognition for Pt^{2+} ions is optimal with G_0.

Compared to these marked dendritic effects, there is no significant dendritic effect for Pd^{2+} ions, which is recognized by the model complex **15** as well as by the dendrimers with approximately the same $\Delta E_{1/2}$ values. This result shows that, of all the metal ions studied, Pd^{II} clearly has the strongest affinity with the 1,2,3-triazole ligand.[13] The titrations reveal a stoichiometry of two 1,2,3-triazole ligands per Pd^{II} (model

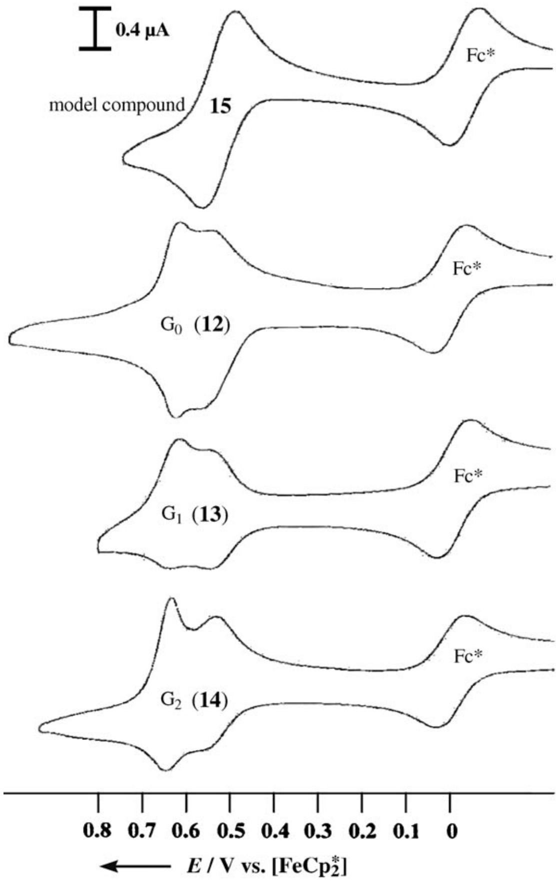

Figure 2. Positive dendritic effect in the titration of Cu^+ ions with dendrimers **12**–**14** compared to the model compound **15**. Cyclovoltammograms of **15** (1.33×10^{-3} M; 1 equiv Cu^+ per branch), **12** (1.26×10^{-4} M; 0.11 equiv Cu^+ per branch), **13** (2.70×10^{-5} M; 0.11 equiv Cu^+ per branch), and **14** (9.0×10^{-6} M; 0.11 equiv Cu^+ per branch). (See Supporting Information for experimental conditions.)

15), although this increases for higher dendrimer generations. This trend also depends on the nature of the metal. For instance, with $[Pd(MeCN)_4](BF_4)_2$ in CH_2Cl_2 the stoichiometry reaches four for **12**, whereas with $[Cu(MeCN)_4](BF_4)$ it is only two for **12**. It is likely that the synergy between the steric constraints and increased number of potential ligands as the dendrimer generation increases disfavors chelation by the 1,2,3-triazole ring and favors the binding of four triazole ligands to each metal center in the large dendrimers. This trend is clearly more drastically marked with the planar geometry of Pd^{II} complexes than with the tetrahedral geometry of Cu^{I} complexes, which can more easily accommodate the three-dimensionality of the intradendritic confinement.

In conclusion, we have synthesized the first click metallodendrimers and shown their use as redox sensors that allow the selective recognition of both oxo anions ($H_2PO_4^-$ and ATP^{2-}) and transition-metal cations with a variety of dramatic dendritic effects.[14] Finally, we show that these easily synthesized composite metallodendrimers with multiple internal heterocyclic ligands clearly offer attractive possibilities for encapsulation, transport, and catalysis.

Experimental Section

General procedure for the click reactions: The azido dendrimer (1 equiv) and the alkyne (1.5 equiv per branch) were dissolved in THF and water was added (1:1, THF/water). At 20°C, $CuSO_4$ (1M aqueous solution, 1 equiv per branch) was added then a freshly prepared solution of sodium ascorbate (1M aqueous solution, 2 equiv per branch) was added dropwise. The solution was then stirred for 30 min at room temperature. After removing THF under vacuum, dichloromethane and an aqueous solution of ammonia were added. The mixture was stirred for 10 min to remove all the Cu^{I} trapped inside the dendrimer as $[Cu(NH_3)_6]^+$ ions. The organic phase was washed twice with water, filtered through celite, and the solvent was removed under vacuum. The product was washed with pentane to remove the excess of alkyne and precipitated by addition of dichloromethane/pentane. The organic dendrimers were obtained as colorless, waxy products and the ferrocenyl dendrimers were obtained as orange, waxy products, usually in high yields in both series. For details of all experimental procedures, characterization data of all products, mass spectra, ^1H NMR spectra, cyclic voltammetry conditions, and voltammograms monitoring the titrations, see the Supporting Information

Received: July 18, 2006

Keywords: anions · cations · dendrimers · ferrocenes · redox chemistry

[1] a) A. W. Bosman, E. W. Jensen, E. W. Meijer, *Chem. Rev.* **1999**, *99*, 1665; b) *Dendrimers and Nanosciences*, (Guest Ed.: D. Astruc), C. R. Chimie, Elsevier, Paris, **2003**, *6*, issues 8–10.

[2] a) A. W. Kleij, A. Ford, J. T. B. H. Jastrzebski, G. van Koten in *Dendrimers and Other Dendritic Polymers* (Eds.: J. M. J. Fréchet, D. A. Tomalia), Wiley, New York, **2002**, p. 185; b) D. Astruc, M.-C. Daniel, J. Ruiz, *Chem. Commun.* **2004**, 2637.

[3] a) R. Huisgen, *Angew. Chem.* **1968**, *80*, 329; *Angew. Chem. Int. Ed. Engl.* **1968**, *7*, 321; b) for a seminal review, see: H. C. Kolb, M. G. Finn, K. B. Sharpless, *Angew. Chem.* **2001**, *113*, 2056; *Angew. Chem. Int. Ed.* **2001**, *40*, 2004; c) V. V. Rostovtsev, L. G. Green, V. V. Fokin, K. B. Sharpless, *Angew. Chem.* **2002**, *114*, 2708; *Angew. Chem. Int. Ed.* **2002**, *41*, 2596; V. D. Bock, H. Hiemstra, J. H. van Maarseveen, *Eur. J. Org. Chem.* **2006**, 51.

[4] a) P. Wu, A. K. Feldman, A. K. Nugent, C. J. Hawker, A. Scheel, B. Voit, J. Pyun, J. M. J. Fréchet, K. B. Sharpless, V. V. Fokin, *Angew. Chem.* **2004**, *116*, 4018; *Angew. Chem. Int. Ed.* **2004**, *43*, 3928; b) M. J. Joralemon, R. K. O'Reilly, J. B. Matson, A. K. Nugent, C. J. Hawker, K. L. Wooley, *Macromolecules* **2005**, *38*, 5436; c) J. W. Lee, B.-K. Kim, *Bull. Korean Chem. Soc.* **2005**, *26*, 658.

[5] G. R. Newkome, Z. Yao, G. R. Baker, V. K. Gupta, *J. Org. Chem.* **1985**, *50*, 2003.

[6] J. Ruiz, G. Lafuente, S. Marcen, C. Ornelas, S. Lazare, J.-C. Blais, E. Cloutet, D. Astruc, *J. Am. Chem. Soc.* **2003**, *125*, 7250.

[7] A. W. van der Made, P. W. N. M. van Leeuwen, J. C. de Wilde, R. A. C. Brandes, *Adv. Mater.* **1993**, *5*, 466.

[8] For a review on ferrocenyl dendrimers and their electrochemical properties, see: C. M. Casado, I. Cuadrado, M. Morán, B. Alonso, B. Garcia, B. Gonzales, J. Losada, *Coord. Chem. Rev.* **1999**, *185–186*, 53.

[9] a) J. B. Flanagan, S. Margel, A. J. Bard, F. C. Anson, *J. Am. Chem. Soc.* **1978**, *100*, 4248; b) A. J. Bard, R. L. Faulkner, *Electrochemical Methods*, 2nd ed., Wiley, New York, **2001**.

[10] P. D. Beer, *Angew. Chem.* **2001**, *113*, 502; *Angew. Chem. Int. Ed.* **2001**, *40*, 486; W. W. H. Wong, D. Curiel, S.-W. Lai, M. G. B. Drew, P. D. Beer, *Dalton Trans.* **2005**, 774.

[11] M. D. Lankshear, A. R. Cowley, P. D. Beer, *Chem. Commun.* **2006**, 612.

[12] S. R. Miller, D. A. Gustowski, Z.-H. Chen, G. W. Gokel, L. Echegoyen, A. E. Kaifer, *Anal. Chem.* **1988**, *60*, 2021.

[13] No comparison of various metal–1,2,3-triazole bond strengths exists to date. For reports of complexes, see: Pd^{II}: M. Barz, E. Herdtweck, W. R. Thiel, *Angew. Chem.* **1998**, *110*, 2380; *Angew. Chem. Int. Ed.* **1998**, *37*, 2262; Pt^{II}: S. Komeda, M. Lutz, A. L. Spek, Y. Yamanaka, T. Sato, M. Chikuma, J. Reedijk, *J. Am. Chem. Soc.* **2002**, *124*, 4738; Cu^{I}: T. R. Chan, R. Hilgraf, K. B. Sharpless, V. V. Fokin, *Org. Lett.* **2004**, *6*, 2853.

[14] For dendritic effects in redox anion recognition, see: C. Valério, J.-L. Fillaut, J. Ruiz, J. Guittard, J.-C. Blais, D. Astruc, *J. Am. Chem. Soc.* **1997**, *119*, 2588; C. M. Casado, I. Cuadrado, B. Alonso, M. Morán, J. Losada, *J. Electroanal. Chem.* **1999**, *463*, 87; B. Alonso, C. M. Casado, I. Cuadrado, M. Morán, A. E. Kaifer, *Chem. Commun.* **2002**, *16*, 1778.